

Recognition and Sensing of Nucleoside Monophosphates by a Dicopper(II) Cryptate

Valeria Amendola, Greta Bergamaschi, Armando Buttafava, Luigi Fabbrizzi,* and Enrico Monzani

Dipartimento di Chimica Generale, Università di Pavia, via Taramelli 12, 27100 Pavia, Italy

Received June 7, 2009; E-mail: luigi.fabbrizzi@unipv.it

Abstract: The dimetallic cryptate $[\text{Cu}_2^{\text{II}}(1)]^{4+}$ selectively recognizes guanosine monophosphate with respect to other nucleoside monophosphates (NMPs) in a MeOH/water solution at pH 7. Recognition is efficiently signaled through the displacement of the indicator 6-carboxyfluorescein bound to the receptor, monitoring its yellow fluorescent emission. Titration experiments evidenced the occurrence of several simultaneous equilibria involving 1:1 and 2:1 receptor/NMP and receptor/indicator complexes. It was demonstrated that the added NMP displaces the indicator from the 2:1 receptor/indicator complex, forming the 1:1 receptor/analyte inclusion complex. Recognition selectivity is thus ascribed to the nature of nucleotide donor atoms involved in the coordination and their ability to encompass the $\text{Cu}^{\text{II}}-\text{Cu}^{\text{II}}$ distance within the cryptate.

Introduction

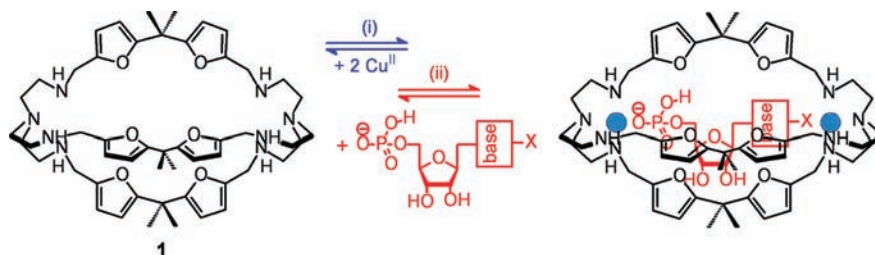
Great attention has been given to the design of fluorescent sensors of nucleoside polyphosphates (NPPs).¹ Such an interest derives from the central role NPPs play in many biological processes. In particular, they provide a universal source of chemical energy (adenosine triphosphate (ATP) and guanosine triphosphate),² participate in cellular signaling (cyclic guanosine monophosphate (GMP) and cyclic adenosine monophosphate (AMP)),³ and are part of important cofactors of enzymatic reactions (coenzyme A, flavin adenine dinucleotide, flavin

mononucleotide, and nicotinamide adenine dinucleotide phosphate).⁴ On the other hand, fluorescence provides the most efficient signal for the quantitative determination of analytes in fluidic media⁵ and, in particular, for the detection in real time and real space of intra- and extracellular substrates.⁶ This feature was first demonstrated through the development of fluorescent sensors for intracellular Ca^{2+} ,⁷ consisting in a semi-dentate chelating agent, inspired by ethylene-glycol-bis(2-aminoethyl ether)-*N,N,N',N'*-tetraacetic acid (EGTA), with a covalently bound fluorogenic moiety,⁸ and was later extended to any kind of substrate of biological relevance.

Typically, recognition of NPPs takes place at the phosphate group, making it a type of anion coordination chemistry. Artificial receptors bind anions by either hydrogen-bonding or metal–ligand interactions.⁹ Hydrogen-bonding interactions are intrinsically weak, and the receptor suffers the competition by water for the anion, which limits investigations to nonaqueous media. Thus, in order to operate under physiological conditions, a receptor's H-bond-donating tendencies have to be enhanced by the presence of positively charged groups. Metal–ligand interactions are in general stronger than H-bond interactions and compete successfully with water for the anion, thus allowing

- (1) (a) Kim, S. K.; Lee, D. H.; Hong, J.-I.; Yoon, J. *Acc. Chem. Res.* **2009**, *42*, 23–31. (b) Ojida, A.; Takashima, I.; Kohira, T.; Nonaka, H.; Hamachi, I. *J. Am. Chem. Soc.* **2008**, *130*, 12095–12101. (c) Kwon, T.-H.; Kim, H. J.; Hong, J.-I. *Chem.—Eur. J.* **2008**, *14*, 9613–9619. (d) Wang, H.; Chan, W.-H. *Org. Biomol. Chem.* **2008**, *6*, 162–168. (e) Ojida, A.; Takashima, I.; Kohira, T.; Nonaka, H.; Hamachi, I. *J. Am. Chem. Soc.* **2008**, *130*, 12095–12101. (f) Oh, D. J.; Ahn, K. H. *Org. Lett.* **2008**, *10*, 3539–3542. (g) Yushchenko, D. A.; Vadzyuk, O. B.; Kosterin, S. O.; Duportail, G.; Mély, Y.; Pivovarenko, V. G. *Anal. Biochem.* **2007**, *369*, 218–225. (h) Zyryanov, G. V.; Palacios, M. A.; Anzenbacher, P. *Angew. Chem., Int. Ed.* **2007**, *46*, 7849–7852. (i) Kumar, S. M. S.; Kim, J. S.; Yoon, J. *Tetrahedron Lett.* **2007**, *48*, 8683–8686. (j) Belin, C.; Astruc, D. *Angew. Chem., Int. Ed.* **2006**, *45*, 132–136. (k) Ojida, A.; Miyahara, Y.; Wongkongkatep, J.; Tamaru, S.-I.; Sada, K.; Hamachi, I. *Chem. Asian J.* **2006**, *1*, 555–563. (l) Pivovarenko, V. G.; Vadzyuk, O. B.; Kosterin, S. O. *J. Fluoresc.* **2006**, *16*, 9–15. (m) Bazzicalupi, C.; Biagini, S.; Bencini, A.; Faggi, E.; Giorgi, C.; Matera, I.; Valtancoli, B. *Chem. Commun.* **2006**, 4087–4089. (n) Wang, S.; Chang, Y.-T. *J. Am. Chem. Soc.* **2006**, *128*, 10380–10381. (o) Aoki, S.; Zulkafeli, M.; Shiro, M.; Kohsako, M.; Takeda, K.; Kimura, E. *J. Am. Chem. Soc.* **2005**, *127*, 9129–9139. (p) Lee, D. H.; Kim, S. Y.; Hong, J.-I. *Angew. Chem., Int. Ed.* **2004**, *43*, 4777–4780. (q) Kwon, J. Y.; Singh, N. J.; Kim, H. N.; Kim, S. K.; Yoon, J. *J. Am. Chem. Soc.* **2004**, *126*, 8892–8893. (r) Urano, Y.; Odani, A.; Kikuchi, K. *J. Am. Chem. Soc.* **2002**, *124*, 3920–3925. (s) Padilla-Tosta, M. E.; Lloris, J. M.; Martínez-Máñez, R.; Pardo, T.; Sancenón, F.; Soto, J.; Marcos, M. D. *Eur. J. Inorg. Chem.* **2001**, 1221–1226. (t) Piantanida, I.; Palm, B. S.; Cudic, P.; Zinica, M.; Schneider, H.-J. *Tetrahedron Lett.* **2001**, *42*, 6779–6783. (u) Schneider, S. E.; O'Neil, S. N.; Ansllyn, E. V. *J. Am. Chem. Soc.* **2000**, *122*, 542–543.
- (2) Nicholls, D. G.; Ferguson, S. J. *Bioenergetics 3*; Academic Press: San Diego, CA, 2002.
- (3) Hancock, J. T. *Cell Signalling*; Longman: Harlow, UK, 1997.

- (4) Metzler D. E.; Metzler, C. M. *Biochemistry: the chemical reactions of living cells*; Harcourt/Academic Press: San Diego, CA, 2003.
- (5) (a) Valeur, B. *Molecular Fluorescence: Principles and Applications*; Wiley-VCH: New York, 2001. (b) Lakowicz, J. R. *Principles of Fluorescence Spectroscopy*, 2nd ed.; Kluwer Academic/Plenum: New York, 1999. (c) Czarnik, A. W. *Fluorescent Chemosensors for Ion and Molecule Recognition*; American Chemical Society: Washington, DC, 1993. (d) Srinivasan, N.; Kilburn, J. D. *Curr. Opin. Chem. Biol.* **2004**, *8*, 305–310. Rurack, K.; Resch-Genger, U. *Chem. Soc. Rev.* **2002**, *31*, 116–127. Valeur, B.; Leray, I. *Coord. Chem. Rev.* **2000**, *205*, 3–40.
- (6) (a) Geddes, C. D.; Lakowicz, J. R. *Topics in Fluorescence Spectroscopy*; Springer: New York, 2005; Vol. 9. (b) Geddes, C. D.; Lakowicz, J. R. *Topics in Fluorescence Spectroscopy*; Springer: New York, 2005; Vol. 10.
- (7) Grynkiewicz, G.; Poenie, M.; Tsien, R. Y. *J. Biol. Chem.* **1985**, *260*, 3440–3450.
- (8) Schmid, R. W.; Reilley, C. N. *Anal. Chem.* **1957**, *29*, 264–268.

Scheme 1. Cascade Process for the Inclusion into the Bistren Cryptand **1** of (i) Two Cu^{II} ions and (ii) a Nucleoside Monophosphate

recognition studies to be carried out in pure water at physiological pH. In fact, a number of NPP receptors that contain Zn^{II} and Cd^{II} ions as binding centers for the phosphate group(s) have been described.^{1e,f,o,p,r} Post-transition Zn^{II} and Cd^{II} metal ions have been chosen because of their redox inactivity and d¹⁰ electronic configuration which prevent any interference with the proximate fluorophore, covalently linked to the coordinating framework, through electron-transfer and energy-transfer processes, respectively.

However, if recognition is designed to occur at the phosphate group, one can expect to discriminate NPP only on the basis of the number of phosphate fragments present, whether one, two, or three, thus exerting linear recognition selectivity. Indeed, several systems capable of discriminating ATP from adenosine diphosphate (ADP) and AMP were described during the past decade. However, no attempts were made to discriminate NPPs on the basis of the nature of the pertinent nucleic base. This may be surprising, because nucleic bases contain potential donor atoms, e.g., sp³ and sp² nitrogen atoms, whose binding tendencies toward transition metals are well established. In this work we describe a dimetallic receptor capable of discriminating nucleoside monophosphates (NMPs) through coordinative interactions at both the phosphonate group and the nucleic base moiety.

The designed receptor derives from the bistren cryptand **1**, which, according to path (i) in Scheme 1, can include two Cu^{II} ions. Each Cu^{II} ion is bound to the four nitrogen atoms of each tren subunits and, being prepared for five-coordination, is prone to interaction with a further donor atom X of the nitrogenous base. Thus, according to path (ii), the cryptate [Cu^{II}₂(**1**)]⁴⁺ is available for interaction with a NMP anion: one Cu^{II} center binds the negatively charged oxygen atom of the phosphonate moiety, and the other interacts with a donor atom of the nucleobase. Signaling profits from the indicator displacement paradigm,¹⁰ choosing 6-carboxyfluorescein as a fluorescent dye. According to this approach, the receptor interacts with a fluorogenic indicator and quenches its emission. The analyte is then added, which forms with the receptor a more stable complex and displaces the indicator. At this stage, the indicator, released to

the bulk solution, can emit its natural fluorescence, thus signaling the establishment of the receptor–analyte interaction. A distinctive discriminating behavior will be demonstrated which derives (i) from the different coordinating tendencies of the donor atoms of each nucleobase toward Cu^{II} and (ii) from the ability of the NMP ion to fit the amplitude of the cryptate's cavity. Investigations were carried out in MeOH/water solution (50:50, v/v), buffered at pH 7. It is anticipated that the two Cu^{II} centers inside the cage have a doubly beneficial effect: (i) they establish strong, yet reversible, coordinative interactions with NMP oxygen and nitrogen donor atoms; and (ii) thanks to their ability to quench any bound fluorophore, they make possible the use of the indicator displacement paradigm, thus allowing NMP recognition to be signaled through a sharp revival of fluorescein emission.

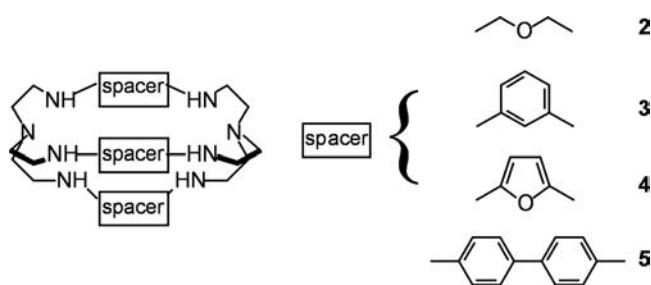
Experimental Section

Instrumentation and Methods. Spectrofluorimetric measurements were performed with a Perkin-Elmer LS 50B instrument, and UV/vis spectra were run on a Varian Cary 1000 SCAN spectrophotometer. The cyclic voltammograms were performed with a BAS 100B/W instrument. The measurements were carried out under oxygen-free conditions using a three-electrode cell. A glassy carbon electrode was the working electrode in the MeOH/H₂O mixture, while a platinum electrode was used in MeCN solvent. A saturated Ag/AgCl electrode was the reference electrode, and platinum wire was used as the auxiliary electrode. The ferrocene/ferrocenium couple (Fc/Fc⁺) was used as an internal standard. pH titrations were carried out with a Radiometer TitraLab 90 titration system. All titrations were performed at 25.0 ± 0.1 °C. Protonation constants of ligand L·6HNO₃ (L = **1**) were determined in a MeOH/water (50:50, v/v) mixture, made 0.05 M in NaNO₃. In a typical experiment, 15 mL of a 5 × 10⁻⁴ M ligand solution was treated with an excess of a 1.0 M HNO₃ standard solution. Titrations were run by addition of 10 μL aliquots of carbonate-free standard 0.1 M NaOH, recording 80–100 points for each titration. Complexation constants were determined by carrying out a similar potentiometric titration experiment, with the additional presence of 2 equiv of Cu^{II}(CF₃SO₃)₂. Prior to each potentiometric titration, the standard electrochemical potential (E°) of the glass electrode was determined in the MeOH/water (1:1) mixture by a titration experiment according to the Gran method.¹¹ Protonation and complexation titration data (emf vs mL of NaOH) were processed with the HyperQuad package,¹² to determine the equilibrium constants (reported in Table 1). The EPR measurements were made on a Bruker X-band EMX/12 spectrometer, equipped with a data station and temperature control. The spectral simulations were made using the Bruker Sinfonia package by adopting an Hamiltonian including the electronic and nuclear Zeeman and dipolar interaction terms with anisotropic g- and hf-tensors. Mass spectra were acquired on

- (9) (a) Sessler, J. L.; Gale, P. A.; Cho, W.-S. *Anion Receptor Chemistry*; Royal Society of Chemistry: Cambridge, UK, 2006. (b) Gale, P. A. *Acc. Chem. Res.* **2006**, *39*, 465–475. (c) Schmidtchen, F. P. *Coord. Chem. Rev.* **2006**, *250*, 2918–2928. (d) Amendola, V.; Esteban-Gómez, D.; Fabbrizzi, L.; Licchelli, M. *Acc. Chem. Res.* **2006**, *39*, 343–353. (e) Davis, A. P. *Coord. Chem. Rev.* **2006**, *250*, 2939–2951. (f) Steed, J. W. *Chem. Commun.* **2006**, 2637–2649. (g) Martínez-Máñez, R.; Sancenón, F. *Chem. Rev.* **2003**, *103*, 4419–4476. (h) Beer, P. D.; Hayes, E. J. *Coord. Chem. Rev.* **2003**, *240*, 167–189. (i) Fabbrizzi, L.; Licchelli, M.; Taglietti, A. *Dalton Trans* **2003**, 3471–3479. (k) McKee, V.; Nelson, J.; Town, R. M. *Chem. Soc. Rev.* **2003**, *32*, 309–325. (l) Beer, P. D.; Gale, P. A. *Angew. Chem., Int. Ed.* **2001**, *40*, 486–516.
- (10) Wiskur, S. L.; Ait-Haddou, H.; Lavigne, J. J.; Anslyn, E. V. *Acc. Chem. Res.* **2001**, *34*, 963–972.

- (11) (a) Gran, G. *Analyst (London)* **1952**, *77*, 661–771. (b) Gans, P.; O'Sullivan, B. *Talanta* **2000**, *51*, 33–37.
- (12) Gans, P.; Sabatini, A.; Vacca, A. *Talanta* **1996**, *43*, 1739–1753. <http://www.hyperquad.co.uk/index.htm>, accessed on July 25, 2009.

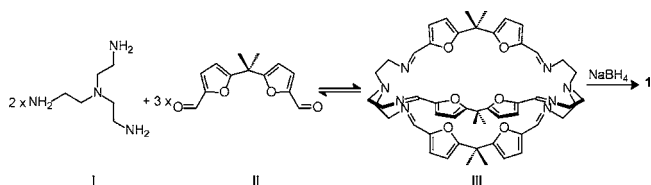
Chart 1. Bistren Cryptands



a Thermo-Finnigan ion-trap LCQ Advantage Max instrument equipped with an ESI source, and NMR spectra were recorded on a Bruker ADVANCE 400 spectrometer.

Spectrofluorimetric Titrations. All spectrofluorimetric titrations were performed in the MeOH/water (1:1) mixture, thermostated at 25 °C and buffered to pH 7 (0.05 M HEPES). Receptor/indicator affinity constants were determined by adding aliquots of a 2.3×10^{-3} M dicopper(II) complex solution to a 2×10^{-7} M solution of 6-carboxyfluorescein. After each addition, the emission spectra of the indicator solution were recorded using a quartz cuvette. Similar titration experiments were performed with each NMP. In a typical titration, aliquots of the NMP solution were added to a 2×10^{-7} M solution of the indicator in the presence of 100 equiv of the dicopper(II) complex $[\text{Cu}_2^{\text{II}}(\mathbf{1})]^{4+}$ (2×10^{-5} M).

Syntheses. All reagents for syntheses were purchased from Aldrich/Fluka and used without further purification. All reactions were performed under dinitrogen. 2,2-Bis(5-formyl-2-furyl)propane (**II**) was prepared as described.¹³



Bistren Cryptand 1. A solution of 2,2-bis(5-formyl-2-furyl)propane (**II**, 1 g, 4.31 mmol) in 150 mL of MeCN was added dropwise to a stirred solution of tris(2-aminoethyl)amine (tren, **I**) (429 μL , 2.87 mmol) in MeCN (100 mL) over 1.5 h at room temperature in an argon atmosphere. After 24 h stirring, the Schiff base **III** formed as a yellowish precipitate, which was filtered out. Then, 1.0 g of the Schiff base **III** was suspended in 150 mL of CH_3OH , heated to 45 °C, and hydrogenated with NaBH_4 (2.3 g). When the addition was complete, the reaction mixture was stirred and refluxed for 2 h. The solvent was then removed, and the residue was dissolved in basic water (40 mL, 6 M NaOH) and extracted with toluene. The collected organic phases were dried over Na_2SO_4 and evaporated to dryness. A light yellow oil was obtained. The oil was dissolved in 20 mL of EtOH, and 65% HNO_3 was added dropwise. The resultant white precipitate ($\mathbf{1} \cdot 6\text{HNO}_3$) was collected on a frit, washed with Et_2O , and dried. ¹H NMR (400 MHz DMSO-*d*₆): 5.9–6.1 (m, 12H, furan ring), 3.55 (s, 12H), 2.45 (br, 24H), 1.52 (s, 18H); ESI-MS *m/z* (+) 894 $[\text{M} + \text{H}]^+$, 447 $[\text{M} + 2\text{H}]^{2+}$. Calcd for $\text{C}_{51}\text{H}_{72}\text{N}_8\text{O}_6 \cdot 6\text{HNO}_3 \cdot 2\text{H}_2\text{O}$: C, 46.86; H, 6.32; N, 15.00. Found: C, 46.79; H, 6.76; N, 14.98.

Results and Discussion

Design Concept. The first dimetallic cryptate complex was obtained with the bistren ligand (**2**, Chart 1) by Lehn,¹⁴ who

used the term “cascade”¹⁵ in order to illustrate the stepwise process by which the octamine cage includes first two transition ions (e.g., Cu^{II}) and then an ambidentate anion (e.g., chloride) capable of bridging the two metal centers.

Each Cu^{II} ion within the cryptate complex reaches its preferred five-coordination in an axially compressed trigonal bipyramidal geometry, through the binding of the four amine nitrogen atoms of each tren subunit and a donor atom of the encapsulated anion (or from a solvent molecule, if the counterion is too large or too poorly coordinating to be included in the cryptate cavity, e.g., ClO_4^- , CF_3SO_3^- , PF_6^-). Later, Lehn and Martell reported equilibrium studies in aqueous solution on the inclusion of F^- and OH^- anions into the cavity of the $[\text{Cu}_2^{\text{II}}(\mathbf{2})]^{4+}$ complex.¹⁶ This investigation showed that, in aqueous media, the OH^- ion can seriously compete for Cu^{II} coordination, which requires accurate pH control. In a more recent investigation, it was shown that the dicopper(II) complex of cryptand **3** (Chart 1), containing rigid 1,3-xylyl spacers, exerted a sharp peak selectivity upon anion inclusion in aqueous neutral solution.¹⁷ In particular, the highest association constant was observed for the N_3^- anion, which exhibits the correct bite length (i.e., the distance between two consecutive donor atoms) for bridging the two Cu^{II} centers, without inducing any rearrangement of the cage framework. On the other hand, an endergonic reorganization of the receptor was observed for anions of smaller (e.g., NO_3^-) or larger bite length (e.g., NCS^-), which exhibited distinctly lower association constants. Quite interestingly, the cryptate complex $[\text{Cu}_2^{\text{II}}(\mathbf{4})]^{4+}$ (Chart 1) was able to establish additional binding interactions with encapsulated Cl^- and Br^- anions through π donor–acceptor interactions involving a filled p orbital of the furan oxygen atom (donor) and an empty $d\pi$ orbital of the halide ion (acceptor), as suggested by the unusually short oxygen–halide distance.¹⁸ Finally, the behavior of the cryptate complex $[\text{Cu}_2^{\text{II}}(\mathbf{5})]^{4+}$ (Chart 1), containing 4,4'-ditolyl spacers, was investigated. Such a cryptate presents an ellipsoidal cavity large enough to include anions with distinct and separate coordinating moieties, e.g., aromatic and aliphatic dicarboxylates. In particular, it was found that $[\text{Cu}_2^{\text{II}}(\mathbf{5})]^{4+}$ exerts geometric selectivity for linear aliphatic carboxylates of general formula $^-\text{OOC}(\text{CH}_2)_n\text{COO}^-$, the highest association constants being observed for $n = 3$ and 4 (glutarate and adipate).¹⁹ On this basis, the cryptate complex $[\text{Cu}_2^{\text{II}}(\mathbf{5})]^{4+}$ could be successfully used for the recognition of the amino acid L-glutamate in the presence of an excess of any other neurotransmitter.²⁰

Bistren cryptands are usually synthesized through Schiff base condensation of 2 mol of tren and 3 mol of the appropriate dialdehyde (Chart 1).²¹ The “reversible” C=N bonds favor the formation of the octamine cage through a trial-and-error

(15) Lehn, J.-M. *Pure Appl. Chem.* **1980**, *52*, 2441–2459.

(16) Motekaitis, R. J.; Martell, A. E.; Murase, I.; Lehn, J.-M.; Hosseini, M. W. *Inorg. Chem.* **1988**, *27*, 3630–3636.

(17) (a) Fabbri, L.; Pallavicini, P.; Perotti, A.; Parodi, L.; Taglietti, A. *Inorg. Chim. Acta* **1995**, *238*, 5–8. (b) Fabbri, L.; Leone, A.; Taglietti, A. *Angew. Chem., Int. Ed.* **2001**, *40*, 3066–3069.

(18) (a) Amendola, V.; Bastianello, E.; Fabbri, L.; Mangano, C.; Pallavicini, P.; Perotti, A.; Manotti Lanfredi, A.; Ugozzoli, F. *Angew. Chem., Int. Ed.* **2000**, *39*, 2917–2920. (b) Amendola, V.; Bergamaschi, G.; Boiocchi, M.; Fabbri, L.; Poggi, A.; Zema, M. *Inorg. Chim. Acta* **2008**, *361*, 4038–4046.

(19) Boiocchi, M.; Bonizzoni, M.; Fabbri, L.; Piovani, G.; Taglietti, A. *Angew. Chem., Int. Ed.* **2004**, *116*, 3935–3940.

(20) Bonizzoni, M.; Fabbri, L.; Piovani, G.; Taglietti, A. *Tetrahedron* **2004**, *60*, 11159–11162.

(21) McDowell, D.; Nelson, J. *Tetrahedron Lett.* **1988**, *29*, 385–386.

(13) Minghu, W.; Enqin, F.; Chengtai, W. *Inorg. Chim. Acta* **1995**, *231*, 217–219.

(14) Motekaitis, R. J.; Martell, A. E.; Dietrich, B.; Lehn, J.-M. *Inorg. Chem.* **1984**, *23*, 1588–1591.

Table 1. Equilibrium Constants for the Protonation and Complexation Equilibria Involving **1** ($= L$) in MeOH/Water (50:50, v/v) at 25 °C^a

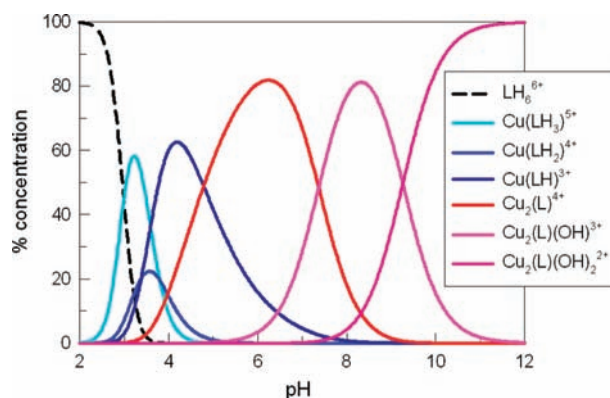
equilibrium	log K
$L + H^+ \rightleftharpoons LH^+$	8.89(1)
$LH^+ + H^+ \rightleftharpoons LH_2^{2+}$	8.51(1)
$LH_2^{2+} + H^+ \rightleftharpoons LH_3^{3+}$	7.49(2)
$LH_3^{3+} + H^+ \rightleftharpoons LH_4^{4+}$	6.89(2)
$LH_4^{4+} + H^+ \rightleftharpoons LH_5^{5+}$	6.17(3)
$LH_5^{5+} + H^+ \rightleftharpoons LH_6^{6+}$	5.21(3)
$L + H^+ + Cu^{2+} \rightleftharpoons [Cu^II(LH)]^{3+}$	30.12(2)
$L + 2H^+ + Cu^{2+} \rightleftharpoons [Cu^II(LH_2)]^{4+}$	33.50(2)
$L + 3H^+ + Cu^{2+} \rightleftharpoons [Cu^II(LH_3)]^{5+}$	30.12(2)
$L + 2Cu^{2+} \rightleftharpoons [Cu_2^II(L)]^{4+}$	33.50(1)
$L + 2Cu^{2+} + H_2O \rightleftharpoons [Cu_2^II(L)((OH))^{3+}] + H^+$	21.53(2)
$L + 2Cu^{2+} + 2H_2O \rightleftharpoons [Cu_2^II(L)((OH)_2)]^{2+} + 2H^+$	12.27(2)

^a In parentheses, the standard deviation on the last figure. Ionic product of water, $pK_w = 13.95$.

mechanism;²² subsequently, carbon–nitrogen bonds are made “irreversible” by hydrogenation with $NaBH_4$. In order to generate an especially large cavity, we chose as a dialdehyde 5,5'-methylidifuran-2-carbaldehyde. The obtained bistren cryptand **1**, due to its longer spacers, is expected to provide an ellipsoidal cavity whose longer axis is greater than that of cage **5**. Moreover, the presence of an sp^3 carbon atom joining the two furan moieties should provide additional flexibility and could make the cavity of the corresponding dimetallic cryptate better able to include the substrate.

Characterization in Solution of the Cryptate Complex $[Cu_2^II(L)]^{4+}$. Equilibrium studies on the formation of the dimetallic cryptate complex were carried out in a water/methanol solution (50:50, v/v). Such a composition ensured full solubility of the investigated systems as well as safe control and instrumental determination of pH. Preliminary experiments were performed in order to determine the acid–base behavior of octamine **1**. In particular, a solution containing **1** and excess strong acid was titrated with a standard water/MeOH solution of NaOH, and pH was measured with a glass electrode. The pH vs volume of NaOH curve was fitted through a nonlinear least-squares procedure, using the HyperQuad program.²³ Best fitting was obtained by assuming the presence at equilibrium of the following species ($L = \mathbf{1}$), on moving from pH 2 to 12: LH_6^{6+} , LH_5^{5+} , LH_4^{4+} , LH_3^{3+} , LH_2^{2+} , LH^+ , and L . Constants of the pertinent protonation equilibria are reported in Table 1.

It is suggested that these protonation equilibria involve the six secondary amine groups of the octamine **1**, as typically observed in bistren systems. Protonation of the two apical tertiary amine groups in the LH_6^{6+} species is made especially unfavorable by electrostatic repulsions and should take place at $pH < 2$. A similar titration experiment was carried out on a solution containing **1**, 2 equiv of $Cu(CF_3SO_3)_2$, and excess acid. Best fitting of the titration curve was obtained by assuming the presence at equilibrium of a variety of metal complex species. In particular, at low pH values, the following species form: $[Cu(LH_3)]^{5+}$, $[Cu(LH_2)]^{4+}$, and $[Cu(LH)]^{3+}$, in which one Cu^{II} ion should occupy one tren compartment, whereas the other compartment should be protonated and should contain three, two, and one secondary ammonium groups. The dimetallic complex $[Cu_2(L)]^{4+}$ is then formed, in which each metal center

**Figure 1.** Distribution diagram of the species present at the equilibrium for a solution 5×10^{-4} M in **1** and 10^{-3} M in Cu^{II} , over the pH range 2–12 ($L = \mathbf{1}$), in MeOH/water (50:50, v/v) at 25 °C.

is bound to a tren subunit, five-coordination being completed by a water molecule. Afterward, on further increasing pH, the complexes $[Cu_2(L)(OH)]^{3+}$ and $[Cu_2(L)(OH)_2]^{2+}$ form, which originate from stepwise deprotonation of the axially bound water molecules. Constants of the complex formation equilibria are reported in Table 1. Figure 1 displays the concentration profiles of the different complex species in a solution 5×10^{-4} M in **1** and 10^{-3} M in Cu^{II} , over the pH range 2–12.

It is observed that the $[Cu_2(L)]^{4+}$ complex reaches its maximum abundance (85%) at pH 6. This species should offer the easiest inclusion by any ambidentate substrate, as only water molecules have to be displaced. However, our studies on nucleotide recognition were carried out in a solution buffered to pH 7. At this pH, the hydroxide-containing complex, $[Cu_2(L)(OH)]^{3+}$, is present at 40%. However, it will be shown that the metal-bound OH^- can be removed without difficulty by incoming anionic substrates. Paradoxically, a pH increase may enhance the ligating tendencies of nucleobases (*vide infra*). In the following, the formula $[Cu_2^II(\mathbf{1})]^{4+}$ will indicate the mixture, at pH 7, of $[Cu_2(L)]^{4+}$ (60%) and $[Cu_2(L)(OH)]^{3+}$ (40%).

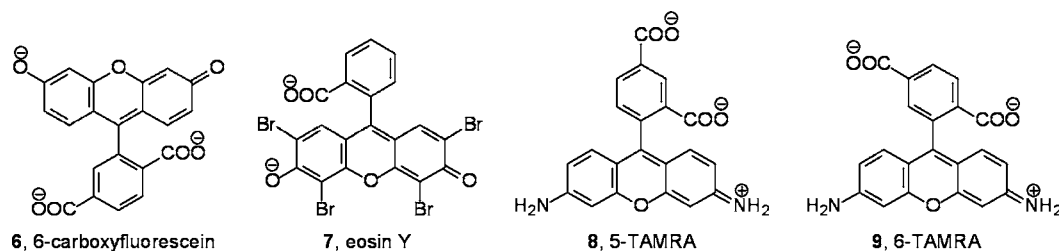
Interaction of Fluorescent Indicators with the Cryptate Complex $[Cu_2^II(\mathbf{1})]^{4+}$. The indicator displacement paradigm (also denoted as “chemosensing ensemble”) was first applied to anion recognition by Anslyn when designing a colorimetric procedure for the detection of citrate in beverages.²⁴ In that case, the indicator was an anionic dye whose color and absorption spectrum drastically changed whether bound to the receptor (which was on its own colorless) or removed from the receptor by the envisaged anion (colorless, too). The color of the dye typically originates from a charge-transfer transition, the dipole intensity of which changes on interaction (electrostatic and/or hydrogen-bonding) with the receptor; a significant change of the absorption properties of the dye occurs on anion binding and recognition. Such a mechanism can operate also in the case of fluorescent dyes, whose emission spectra can be altered by the interaction with the receptor. However, things are made simpler when the binding site of the receptor is a transition metal ion. In fact, the d^n metal center ($n = 1-9$) quenches the excited state of the dye through either an electron-transfer or an energy-transfer process.²⁵ As a consequence, the recognition of the anionic analyte is signaled by the restoration of the fluorescence

(22) Meyer, C. D.; Joiner, C. S.; Stoddart, J. F. *Chem. Soc. Rev.* **2007**, *36*, 1705–1723.

(23) Gans, P.; Sabatini, A.; Vacca, A. *Talanta* **1996**, *43*, 1739–1753. <http://www.hyperquad.co.uk/index.htm>, accessed on July 25, 2009.

(24) (a) Metzger, A.; Lynch, V. M.; Anslyn, E. V. *Angew. Chem., Int. Ed. Engl.* **1997**, *36*, 862–864. (b) Metzger, A.; Anslyn, E. V. *Angew. Chem., Int. Ed.* **1998**, *37*, 649–652.

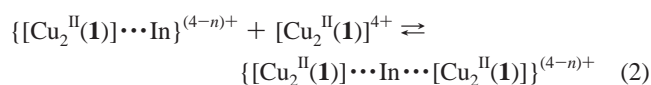
Chart 2. Fluorescent Indicators Tested in This Study



of the indicator released to the solution, according to a well-defined on/off response.

In order to ensure selectivity, the indicator should form with the receptor a rather stable complex. If the dimetallic cryptate $[\text{Cu}_2^{\text{II}}(\mathbf{1})]^{4+}$ is used as a receptor, the indicator should provide two anionic binding sites. This is the case observed for most fluorescent dyes, which possess carboxylate and/or phenolate functional groups. In particular, we considered the anionic indicators **6–9** (Chart 2), and we investigated their affinity toward $[\text{Cu}_2^{\text{II}}(\mathbf{1})]^{4+}$ through spectrofluorimetric titration experiments.

Figure 2a displays the family of emission spectra recorded over the course of the titration of a solution of MeOH/H₂O (50:50) 2×10^{-7} M in the indicator 6-carboxyfluorescein (**6**) and adjusted to pH 7 with HEPES buffer, with a solution 2.3×10^{-3} M in the $[\text{Cu}_2^{\text{II}}(\mathbf{1})]^{4+}$ receptor (obtained by mixing 1 equiv of **1** and 2 equiv of $\text{Cu}(\text{CF}_3\text{SO}_3)_2$). On cryptate addition, the fluorescence of the fluorescein dye is progressively quenched, which reflects the interaction with the metal center(s) of the receptor. The extent of fluorescence quenching is illustrated by the titration profile (symbols in Figure 2b). It is observed that complete quenching of the indicator's fluorescence takes place on addition of more than 100 equiv of the receptor, a consequence of the rather high dilution of the solution. Best fitting of the spectrofluorimetric data over the 500–560 nm range was obtained by assuming the formation of *two* receptor–indicator complex species of 1:1 and 2:1 stoichiometry, as described by equilibria 1 and 2:



The values of the corresponding equilibrium constants are shown in Table 2. It is assumed that, at pH 7, in the presence of the dicopper complex, all the acidic groups of 6-carboxy-

fluorescein (carboxylic and phenolic) are deprotonated;²⁶ thus the indicator detains a triply negative charge: In^{3-} .

From the binding constants K_{F1} and K_{F2} , the concentrations (in %) of the species present at equilibrium over the course of the titration experiment could be calculated, and they are reported in Figure 2b. It is observed that, on addition of the first aliquots of the $[\text{Cu}_2^{\text{II}}(\mathbf{1})]^{4+}$ receptor to the solution of fluorescent indicator **6**, i.e., in the presence of an excess of indicator In^{3-} , a complex of stoichiometry 1:1 (receptor/indicator) forms, $\{[\text{Cu}_2^{\text{II}}(\mathbf{1})] \cdots \text{In}\}^+$, in which the indicator In^{3-} should be included (or partially included) into the cryptate. On further addition of $[\text{Cu}_2^{\text{II}}(\mathbf{1})]^{4+}$, a 2:1 complex forms, $\{[\text{Cu}_2^{\text{II}}(\mathbf{1})] \cdots \text{In} \cdots [\text{Cu}_2^{\text{II}}(\mathbf{1})]\}^{5+}$, in which a carboxyfluorescein anion binds one Cu^{II} center from a cryptate and a second Cu^{II} center from another cryptate, acting as a bridge. The two-step process is illustrated in Scheme 2.

Quite interestingly, the decreasing profile of fluorescence intensity at 516 nm in Figure 2a superimposes well on the decreasing concentration profile of In^{3-} . Noticeably, at the rather low indicator concentration in the titration experiment, the 1:1 inclusion complex reaches the maximum concentration of ca. 30%; on addition of excess receptor, the indicator leaves the receptor's cavity and goes to bridge two Cu^{II} centers of two different cryptates. The fact that $\log K_2 > \log K_1$ may be related to a conformational change of the receptor when the indicator moves from $\{[\text{Cu}_2^{\text{II}}(\mathbf{1})] \cdots \text{In}\}^+$ to $\{[\text{Cu}_2^{\text{II}}(\mathbf{1})] \cdots \text{In} \cdots [\text{Cu}_2^{\text{II}}(\mathbf{1})]\}^{5+}$, and this will be discussed later.

Among the other investigated fluorescent dyes, eosin Y (**7**) shows a $\log K_1$ value close to that of carboxyfluorescein (**6**). Eosin Y possesses just two donor atoms that can be involved in the interaction with the two metal centers: one oxygen atom from the carboxylate group and one oxygen atom from the phenolate group. It is suggested that also 6-carboxyfluorescein coordinates the two Cu^{II} ions within the cryptate cavity by a carboxylate and by a phenolate oxygen atom, which could

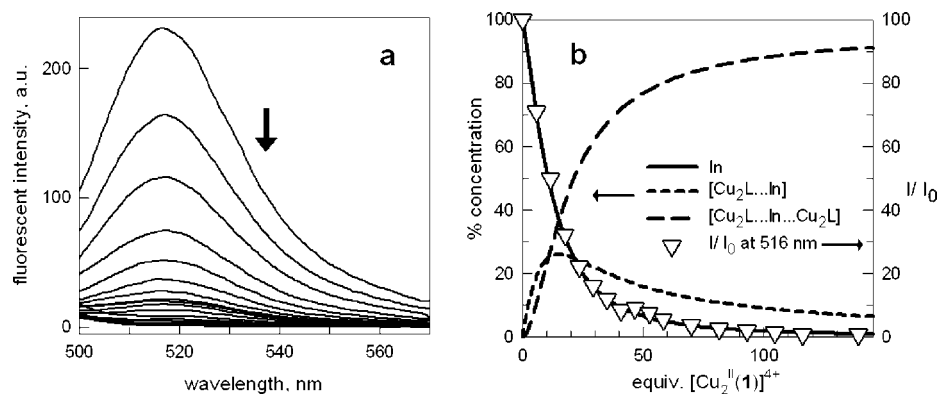


Figure 2. (a) Emission spectra recorded over the course of the titration of a solution of MeOH/H₂O (50:50) 2×10^{-7} M in the indicator 6-carboxyfluorescein (**6**), adjusted to pH 7 with HEPES buffer, with a solution 2.3×10^{-3} M in $[\text{Cu}_2^{\text{II}}(\mathbf{1})]^{4+}$ ($\lambda_{\text{exc}} = 492$ nm); (b) Lines, concentration profiles of the species present at the equilibrium, left vertical axis; symbols, normalized intensity of the emission at 516 nm, right vertical axis.

Table 2. Log K Values for the Equilibria Involving the Receptor $\{[Cu_2^{II}(1)] \cdots In\}^{(4-n)+}$ and a Fluorescent Indicator In^{n-} , in a MeOH/Water Solution (50:50, v/v), Buffered at pH 7, at 25 °C^a

equilibrium at pH 7		indicator			
		6	7	8	9
(1)	$\log K_{F1}$	5.37(1)	5.24(1)	4.56(1)	4.59(1)
(2)	$\log K_{F2}$	5.7(1)	4.38(5)	4.21(4)	4.15(4)

^a In parentheses, standard deviation on the last figure.

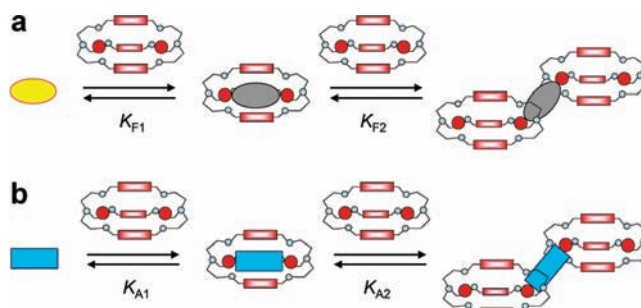
account for the similar $\log K_1$ values. Coordination by the two carboxylate oxygen atoms of the 1,4-benzenedicarboxylate fragment of **6** has to be ruled out for two main reasons: (i) spectrofluorimetric titration experiments have shown that the terephthalate ion (partially) displaces **6** from the $[Cu_2^{II}(1)]^{4+}$ complex, only if added in 100-fold excess, indicating the formation of a much less stable complex, and (ii) the “bite” of the 1,4-benzenedicarboxylate fragment seems too small to encompass the $Cu^{II}-Cu^{II}$ distance in the cryptate cavity, as suggested by molecular modeling. Dyes **8** and **9** form less stable 1:1 inclusion complexes than **6** and **7**, probably because they can bind the two metal centers only by using the benzenedicarboxylate moiety. Moreover, binding of **8** and **9** may profit from a less favorable electrostatic contribution, due to the presence of a less negative overall electrical charge (In^-). As observed for **6**, also dyes **7–9**, in the presence of an excess of $[Cu_2^{II}(1)]^{4+}$, give rise to the 2:1 receptor/indicator complex of general formula $\{[Cu_2^{II}(1)] \cdots In \cdots [Cu_2^{II}(1)]\}^{(8-n)+}$. However, for the latter dyes, the “normal” trend is observed: $\log K_1 > \log K_2$. In this connection, steric effects may play a significant role: in particular, intercage repulsions should disfavor the formation of the 2:1 complex, $\{[Cu_2^{II}(1)] \cdots In \cdots [Cu_2^{II}(1)]\}^{(8-n)+}$.

Interaction of Nucleoside Monophosphates with Receptor $[Cu_2^{II}(1)]^{4+}$. The interaction of NMPs with receptor $[Cu_2^{II}(1)]^{4+}$ was investigated in a MeOH/water (1:1 v/v) solution at pH 7, taking profit from the indicator displacement paradigm and using 6-carboxyfluorescein (**6**) as a fluorescent indicator. Figure 3a shows the emission spectra recorded over the course of a typical spectrofluorimetric titration experiment.

The solution was 2×10^{-5} M in $[Cu_2^{II}(1)]^{4+}$ and 2×10^{-7} M in **6** and was titrated with a standard MeOH/water solution of GMP. On addition of the NMP, the emission band of 6-carboxyfluorescein, centered at 516 nm, began to develop, following the release of In^{3-} from the receptor–indicator complexes ($\{[Cu_2^{II}(1)] \cdots In \cdots [Cu_2^{II}(1)]\}^{5+}$ and $\{[Cu_2^{II}(1)] \cdots In\}^{2+}$), while the receptor–GMP complex, $\{[Cu_2^{II}(1)] \cdots GMP\}^{2+}$, formed. Notice that emission spectra have been normalized with respect to the spectrum of the uncomplexed indicator, measured under the same conditions and reported as a dashed line in Figure 3a. Figure 3b shows the titration profile based on the emission intensity at 516 nm: it is observed that, on addition of 30 equiv of GMP (with respect to $[Cu_2^{II}(1)]^{4+}$), the emission spectrum of 6-carboxyfluorescein has reached ca. 80% of its limiting value; i.e., ca. 80% of the indicator has been removed from the $\{[Cu_2^{II}(1)] \cdots In \cdots [Cu_2^{II}(1)]\}^{5+}$ complex. Similar titration experiments were carried out with other NMPs, and pertinent titration profiles at 516 nm are displayed in Figure 4.

In all cases, the amount of displaced indicator after excess addition of NMP was significantly lower than in the case of GMP, indicating that receptor $[Cu_2^{II}(1)]^{4+}$ exerts a marked selectivity in favor of the latter NMP. Such an effect has to be

Scheme 2. Pictorial Sketch of the Stepwise Equilibria for the Interaction of Receptor $[Cu_2^{II}(1)]^{4+}$ (a) with the Fluorescent Indicator (e.g., Carboxyfluorescein, **6**) and (b) with the Nucleoside Monophosphate^a



^a In (a), following the interaction with the two metal ions, the yellow fluorescence of the indicator (yellow oval) is lost (gray oval). In (b) the NMP molecule (blue rectangle) interacts first with two metal ions of a single cage, and then it leaves the receptor’s cavity and goes to bridge two metal centers of two distinct cryptates. Such a process may induce a beneficial relief of steric constraints.

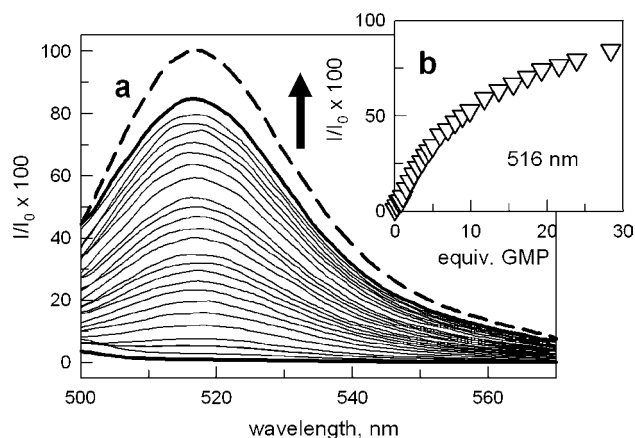


Figure 3. (a) Emission spectra taken over the course of the titration of a 50:50 MeOH/H₂O solution 1.99×10^{-5} M in $[Cu_2^{II}(1)]^{4+}$ and 2×10^{-7} M in **6**, adjusted to pH 7 with HEPES buffer, with a solution of GMP ($\lambda_{exc} = 492$ nm). (b) Emission intensity at 516 nm, normalized with respect to the emission of the free indicator (whose spectrum is given by the dashed line in panel a).

related to the stability of the receptor–NMP complex. In particular, the stability should decrease according to the sequence



Selective interaction is typically associated with a more or less favorable geometrical and binding complementarity between the analyte and the concave receptor, a statement on which the design of receptors for any kind of substrate is based.²⁷ However, selectivity has to be correctly discussed in terms of thermodynamic stability, which, in turn, requires (i) the definition of the receptor–analyte equilibrium (or equilibria) and (ii) the careful determination of pertinent equilibrium constant(s).

- (25) (a) Fabbrizzi, L.; Marcotte, N.; Stomeo, F.; Taglietti, A. *Angew. Chem., Int. Ed.* **2002**, *41*, 3811–3814. (b) Ansa-Hortalá, M.; Fabbrizzi, L.; Marcotte, N.; Stomeo, F.; Taglietti, A. *J. Am. Chem. Soc.* **2003**, *125*, 20–21.
- (26) Aschi, M.; D’Archivio, A. A.; Fontana, A.; Formiglio, A. *J. Org. Chem.* **2008**, *73*, 3411–3417.
- (27) Schneider, H.-J.; Yatsimirsky, A. K. *Chem. Soc. Rev.* **2008**, *37*, 263–277.

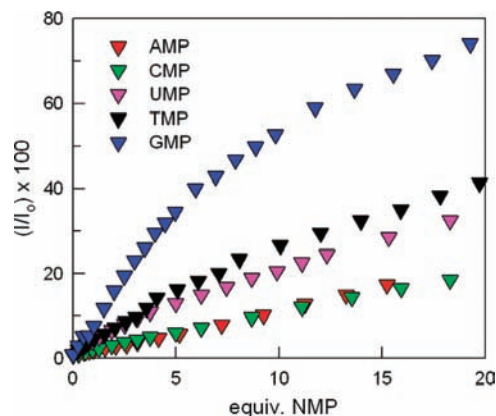
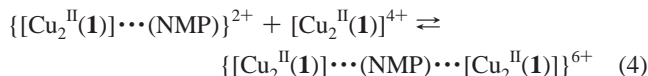


Figure 4. Spectrofluorimetric titration profiles obtained for different nucleoside monophosphates (NMPs) by monitoring the displacement of the indicator **6** from the receptor $[\text{Cu}_2^{\text{II}}(\mathbf{1})]^{4+}$. A 50:50 MeOH/ H_2O (v/v) solution 2×10^{-5} M in $[\text{Cu}_2^{\text{II}}(\mathbf{1})]^{4+}$ and 2×10^{-7} M in **6**, adjusted to pH 7 with HEPES buffer, was titrated with a solution of the chosen NMP. The emission intensity at 516 nm has been normalized with respect to the emission of the uncomplexed indicator.

The equilibria that form the basis of the titration experiments (Figures 3 and 4) and provide the best fit of spectrofluorimetric data (*vide infra*) are (1) and (2), previously investigated and involving the interaction of the receptor with the fluorescent indicator, and (3) and (4), which refer to the interaction of the receptor with the analyte (e.g., the nucleotide GMP):



The determination of the constants of equilibria (3) and (4), K_{A1} and K_{A2} , respectively, from spectrofluorimetric data is not straightforward. In fact, a simple nonlinear least-squares fitting of a titration profile based on a quantity (fluorescent intensity) not directly related to the receptor/NMP complexes may be an unsafe procedure and can lead to the determination of questionable values of K_{A1} and K_{A2} . Thus, a different procedure was chosen, in which the indefiniteness of the system has been reduced on the basis of some reasonable assumptions (see Experimental Part in Supporting Information).

Figure 5 reports the concentrations of the species present at the equilibrium over the course of the titration, calculated from

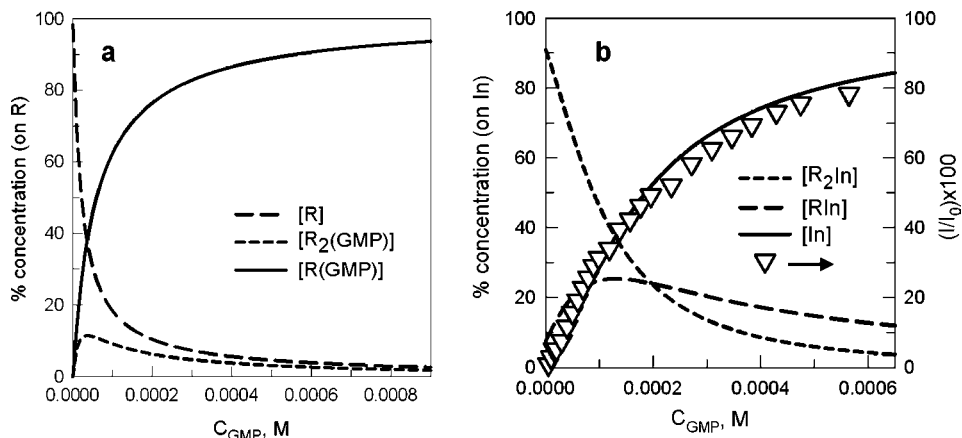


Figure 5. (a) Concentration profiles of the species present at equilibrium, in the spectrofluorimetric titration experiment illustrated in Figure 3; concentration (in %) is referred to the total concentration of the receptor $\text{R} (= [\text{Cu}_2^{\text{II}}(\mathbf{1})]^{4+})$; 2.0×10^{-5} M. (b) Concentration (in %) is referred to the total concentration of the Indicator $\text{In} (= \mathbf{6})$; 2.0×10^{-7} M. Symbols: normalized intensity of the emission at 516 nm of the released indicator, right vertical axis.

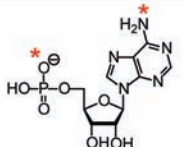
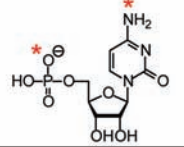
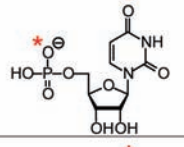
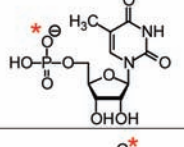
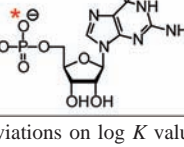
the values of K_{F1} , K_{F2} , K_{A1} , and K_{A2} . In particular, Figure 5a shows how the concentrations of the different forms of the receptor $[\text{Cu}_2^{\text{II}}(\mathbf{1})]^{4+} = \text{R}$ (whether uncomplexed, $[\text{R}]$, or complexed by the analyte, $[\text{R}_2(\text{GMP})]$ and $[\text{R}(\text{GMP})]$) vary on addition of GMP. The concentrations are given in % and are referred to the analytical concentration of R . In the same way, Figure 5b displays the changes of the concentration of the different forms of the fluorescent indicator In , whether complexed by the receptor, $[\text{R}_2\text{In}]$ and $[\text{RIn}]$, or free, $[\text{In}]$. In this case, % concentrations have been calculated with respect to the analytical concentration of In , which is 100-fold lower than that of R (for this reason, $[\text{R}]$, $[\text{R}_2(\text{GMP})]$ and $[\text{R}(\text{GMP})]$, on one side, and $[\text{R}_2\text{In}]$ and $[\text{RIn}]$ and $[\text{In}]$, on the other, were considered in different diagrams, a and b).

Let us consider first the progress of the titration “from the point of view” of the receptor R (Figure 5a). Prior to the first addition of GMP, the receptor exists mostly in the free form R , with only 1% of it complexed with the indicator. Figure 5b indicates that this 1% exists as 90% as R_2In (or $\{[\text{Cu}_2^{\text{II}}(\mathbf{1})] \cdots \text{In} \cdots [\text{Cu}_2^{\text{II}}(\mathbf{1})]\}^{5+}$) and 10% as RIn (or $\{[\text{Cu}_2^{\text{II}}(\mathbf{1})] \cdots \text{In}\}^+$). On GMP addition, the 1:1 complex $\text{R}(\text{GMP})$ (or $\{[\text{Cu}_2^{\text{II}}(\mathbf{1})] \cdots (\text{GMP})\}$) and the 2:1 complex $\text{R}_2(\text{GMP})$ (or $\{[\text{Cu}_2^{\text{II}}(\mathbf{1})] \cdots (\text{GMP}) \cdots [\text{Cu}_2^{\text{II}}(\mathbf{1})]\}^{5+}$) form almost simultaneously (see Figure 5a). However, after the addition of the first aliquots of GMP, the concentration of the $\text{R}_2(\text{GMP})$ complex, which has reached its maximum at 10%, begins to decrease, while the concentration of the 1:1 complex $\text{R}(\text{GMP})$ increases to asymptotically attain 100%. On the other hand, looking at Figure 5b, it is seen that, on GMP addition, the concentration of R_2In decreases, that of RIn increases up to a maximum of 25%, then decreases, and, most importantly, the concentration of the free indicator In , displaced from the complexes by GMP, increases monotonously. Quite interestingly, the normalized emission intensity (triangles in Figure 5b) superimposes satisfactorily on the normalized concentration of the uncomplexed indicator In .

Similar behavior was observed for all the other investigated NMPs. In particular, the formation of the $\text{R}_2(\text{NMP})$ and $\text{R}(\text{NMP})$ complexes was observed. Pertinent equilibrium constant K_{A1} and K_{A2} are reported in Table 3.

Direct evidence of the formation of a stable 1:1 complex between the receptor and GMP is provided by ESI mass studies. Figure 6 shows some details of a spectrum taken on a solution 1.0×10^{-3} M of the receptor containing a 4-fold excess of GMP. In particular, panel (a) displays a double positively charged peak

Table 3. Log *K* Values for the Equilibria (3) (log *K*_{A1}) and (4) (log *K*_{A2})^a

NMP	formula of the nucleotide	log <i>K</i> _{A1}	log <i>K</i> _{A2}
AMP		3.7	4.3
CMP		3.7	4.3
UMP		4.0	4.7
TMP		4.2	4.5
GMP		4.7	4.4

^a Standard deviations on log *K* values are ± 0.1 . MeOH/water solution (50:50, v/v), buffered at pH 7 with HEPES, 25 °C. Red stars indicate the hypothesized donor atoms involved in the coordination to the two Cu^{II} centers inside the cryptate.

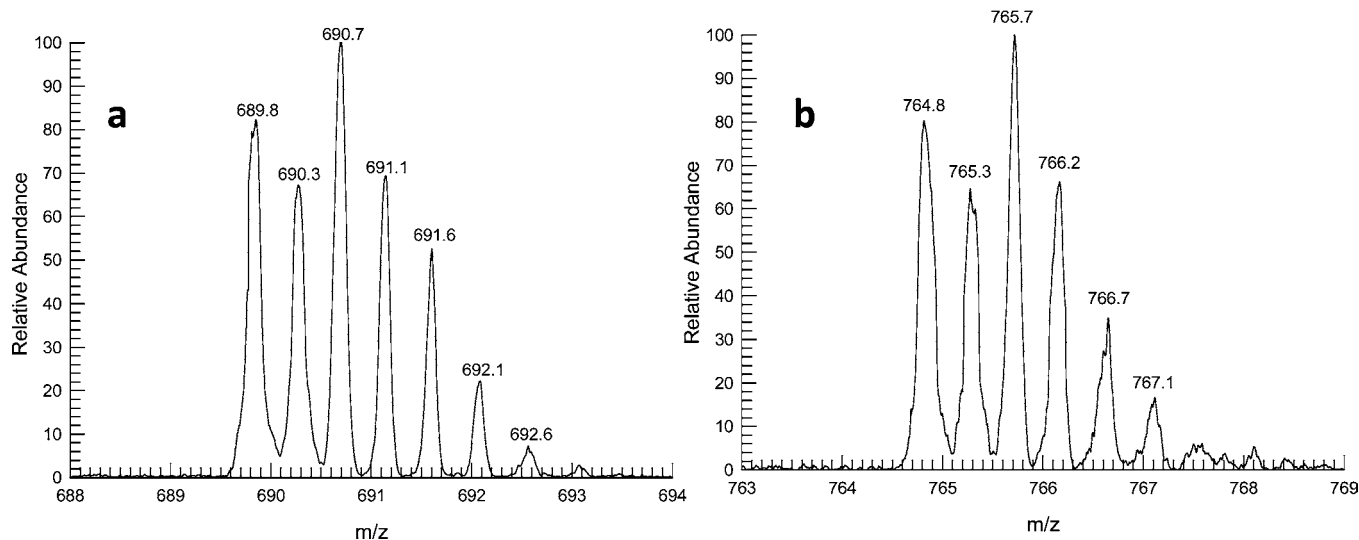
at 690.6 *m/z*, corresponding to the species [Cu₂^{II}(1)(GMP)]²⁺. The isotope pattern confirms the presence of two Cu^{II} ions, while the peak-to-peak separation of 0.5 *m/z* indicates the presence of a double-positive charge of the complex.

On the other hand, panel (b) shows a peak at 765.5 *m/z*, corresponding to the complex species {[Cu₂^{II}(1)GMPH]³⁺, CF₃SO₃⁻]²⁺, in which GMP is monoprotonated and the overall

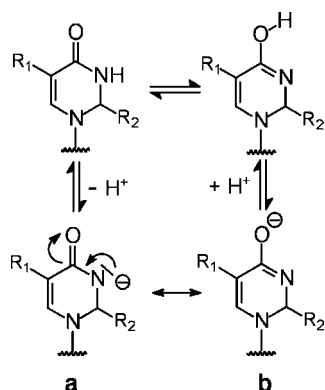
charge is 2+. Simulated spectra are reported in Supporting Information, Figure S7. In contrast, the spectrum taken in the presence of a 4-fold excess of AMP showed only the peak corresponding to plain receptor, without any included nucleotide. This confirms the poor stability of the [Cu₂^{II}(L)(AMP)]²⁺ complex.

Further evidence of the interaction between receptor [Cu₂^{II}(1)]⁴⁺ and nucleotides was sought through electrochemical and ESR studies. In particular, cyclic voltammetry studies were carried out with a glassy carbon working electrode on a MeOH/H₂O (1:1 v/v) solution 1×10^{-3} M in [Cu₂^{II}(1)]⁴⁺, 0.05 M in [Bu₄N]NO₃ and buffered to pH 7 with 0.05 M HEPES. A poorly defined irreversible wave was observed on reduction (see Figure S8 in Supporting Information). Addition of an excess of GMP did not induce any modification of the CV profile. Such a behavior can be ascribed to the poor reversibility of the reduction process at the glassy carbon electrode. Thus, the same experiment was carried in an MeCN solution (0.1 M in [Bu₄N]PF₆) using a platinum working electrode. In the absence of nucleotide, two defined irreversible reduction peaks, at about -450 mV and -600 mV vs Fc⁺/Fc, were observed (see Figure S9 in Supporting Information). However, on addition of even sub-stoichiometric amounts of nucleotide precipitation occurred. More significant results were obtained from ESR studies. In fact, the EPR spectrum of a frozen H₂O:MeOH solution 1×10^{-3} M in [Cu₂^{II}(1)]⁴⁺, buffered to pH 7 with HEPES 0.05 M (see Figure S11 in the Supporting Information) shows a trigonal pattern, with *g*_x = 2.105, *g*_y = 2.110, *g*_z = 2.295, which is consistent with the presence of two equivalent Cu^{II} centers with a trigonal bipyramidal coordination geometry, with a water molecule occupying an apical position. A hyperfine interaction with a nitrogen atom on the *x* component is also observed with *A*_x = 30 G. On the other hand, the spectrum of the same solution containing 4 equiv of GMP shows a rhombic structure, with *g*_x = 2.017, *g*_y = 2.025, *g*_z = 2.220, with *A*_z = 154 G (see Figure S12 in the Supporting Information). Such a pattern is indicative of a pronounced distortion of the trigonal bipyramidal geometry toward a square pyramidal one, which may be induced by the coordination of the NMP.

The diagram based on R (Figure 5a), as well as those referring to other NMPs, demonstrates that the significant receptor/analyte complex that forms over the course of the titration is that of

**Figure 6.** ESI mass spectrum of a solution containing [Cu₂^{II}(1)]⁴⁺ and a 4-fold excess of GMP.

Scheme 3. The Keto-Enolic Tautomeric Equilibrium in the 2,3-Dihydropyrimidin-1-one Ring, Which May Take Place in UMP, TMP, and $\text{GMP}^{28\text{a}}$



^a On deprotonation of the amide N–H fragment, the negative charge moves through a π mechanism from the nitrogen atom (keto form a) to the oxygen atom (enolate form b). The enolate form is stabilized by the coordination to the Cu^{II} center.

1:1 stoichiometry, $\text{R}(\text{NMP})$, and, therefore, the selectivity observed in the spectrofluorimetric response, (shown in Figure 4) is essentially related to the more or less intense interactions established between $[\text{Cu}_2^{\text{II}}(\mathbf{1})]^{4+}$ and NMP within the 1:1 receptor/analyte complex. In fact, data in Table 3 show that the sequence of $\log K_{\text{A1}}$ values parallels the sequence of the fluorescence revival.

At this stage, a rationale for accounting for the stability sequence of 1:1 receptor–NMP complexes should be, at least tentatively, proposed. It is suggested that two main factors determine complex stability: (i) the nature of NMP donor atoms coordinated to the Cu^{II} centers of the receptor and (ii) the capability of NMP to encompass with its donor atoms the $\text{Cu}^{\text{II}}-\text{Cu}^{\text{II}}$ distance inside the cryptate–nucleotide complex. In this connection, it is suggested that nucleotides forming the less stable 1:1 complexes, AMP and CMP, bind the two Cu^{II} centers within the cage by using the convergent $\text{P}-\text{O}^{\ominus}$ (phosphonate, negatively charged) and N–H (aniline, neutral) groups. On the other hand, UMP, TMP and GMP, which all possess an acidic amide N–H fragment, may employ a donor atom of the nucleobase bearing a partial negative charge, thus exhibiting enhanced coordinating tendencies with respect to AMP and CMP. In fact, it is suggested that, at pH 7 and in the presence of a metal center, deprotonation of the N–H amide fragment of 2,3-dihydropyrimidin-1-one ring takes place. The negative charge is then delocalized onto the $\text{C}=\text{O}$ fragment, according to the π mechanism outlined in the keto–enolic tautomeric equilibrium in Scheme 3. Thus, two formally negatively charged groups, $\text{P}-\text{O}^{\ominus}$ and the enolate $\text{C}-\text{O}^{\ominus}$ fragment, can converge to bind the two Cu^{II} ions within the bistren cage.

The appreciably higher stability of the 1:1 complex of GMP with respect to UMP and TMP may be tentatively ascribed to geometrical complementarity effects. Unfortunately, we were not able to obtain crystals of any salt containing either the $[\text{Cu}_2^{\text{II}}(\mathbf{1})]^{4+}$ cation or the nucleotide inclusion complex, suitable for X-ray diffraction studies and we cannot therefore have a precise information on the structural features associated to the complexation process. However, detailed crystallographic structural data are available for the investigated nucleotides. In

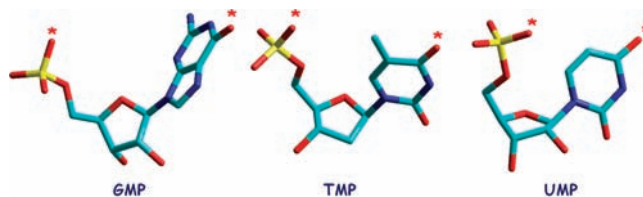


Figure 7. Molecular structures of nucleoside monophosphates. Structures rendered with HyperChem 8, from data deposited at the Cambridge Crystallographic Data Centre. Hydrogen atoms have been omitted for clarity. Red stars label the convergent oxygen donor atoms which may be involved in the coordination of the two Cu^{II} ions within the cryptate complex $[\text{Cu}_2^{\text{II}}(\mathbf{1})]^{4+}$. GMP (guanosine monophosphate), ref 29; TMP (thymidine monophosphate), ref 30; UMP (uridine monophosphate), ref 31.

particular, Figure 7 shows the tube representations of the structures of X-ray investigated NMPs (nuclear coordinates taken from Cambridge Crystallographic Centre).

It is observed that the distances between donor atoms labeled with a star in the formulas reported in Table 3 are as follow: GMP, 8.3 Å;²⁹ TMP, 6.75 Å;³⁰ UMP, 6.0 Å.³¹ On the other hand, the structure of the “empty” receptor $[\text{Cu}_2^{\text{II}}(\mathbf{1})]^{4+}$ was calculated through MM^+ (see Figure S10 in Supporting Information). In particular, we considered the complex in which each Cu^{II} center has an OH^- ion bound in the remaining apical position. The calculated distance between OH^- oxygen atoms is 8.4 Å. Such a value compares well with the X-ray observed distance for GMP donor atoms. Thus, it would appear that GMP forms the most stable inclusion complex because its donor atoms fit receptor’s cavity without inducing any endothermic rearrangement. Such an unfavorable contribution should be present with TMP and UMP, which exhibit a distinctly smaller distance between donor atoms. However, in the absence of X-ray data, this interpretation must be considered entirely speculative.

$\log K_{\text{A2}}$ values for all NMPs range over the 4.3–4.7 interval, thus not showing any pronounced selectivity trend as for $\log K_{\text{A1}}$ values. This seems a quite reasonable behavior, considering that in the 2:1 receptor/NMP complexes the nucleotide bridges the Cu^{II} centers of two different cryptates and should not experience any serious effect of geometrical complementarity. Very interestingly, only in the case of GMP, $\log K_{\text{A1}} > \log K_{\text{A2}}$, whereas for all the other NMPs the opposite occurs ($\log K_{\text{A1}} < \log K_{\text{A2}}$). In this connection, it should be considered that in all 1:1 complexes, except that of GMP, some steric constraints exist, which originate from the misfit between receptor’s cavity and nucleotide, as discussed before. Such constraints are removed, or significantly reduced, on going from the $\{[\text{Cu}_2^{\text{II}}(\mathbf{1})] \cdots (\text{NMP})\}^{2+}$ complex to the $\{[\text{Cu}_2^{\text{II}}(\mathbf{1})] \cdots (\text{NMP}) \cdots [\text{Cu}_2^{\text{II}}(\mathbf{1})]\}^{6+}$ complex, in which the nucleotide bridges two Cu^{II} centers of two distinct cryptates, as illustrated in Scheme 2. It is therefore suggested that it is the beneficial effect associated with strain relief that makes $\log K_{\text{A2}}$ greater than $\log K_{\text{A1}}$. Clearly, such an effect should not operate in the case of GMP, for which a perfect fit within the cavity has been hypothesized.

A Preliminary Look at the Interaction of Other Phosphates with Receptor $[\text{Cu}_2^{\text{II}}(\mathbf{1})]^{4+}$. We were interested to preliminarily consider the interaction of the investigated receptor $[\text{Cu}_2^{\text{II}}(\mathbf{1})]^{4+}$ with phosphates of varying complexity, including inorganic

(28) Kosenkov, D.; Gorb, L.; Shishkin, O. V.; Šponer, J.; Leszczynski, J. *J. Phys. Chem. B* **2008**, *112*, 150–157.

(29) Yajima, T.; Maccarrone, G.; Takani, M.; Contino, A.; Arena, G.; Takamido, R.; Hanaki, M.; Funahashi, Y.; Odani, A.; Yamauchi, O. *Chem.–Eur. J.* **2003**, *9*, 3341–3352.

(30) Trueblood, K. N.; Horn, P.; Luzzati, V. *Acta Crystallogr.* **1961**, *14*, 965–982.

(31) Shefter, E.; Trueblood, K. N. *Acta Crystallogr.* **1965**, *18*, 1067–1077.

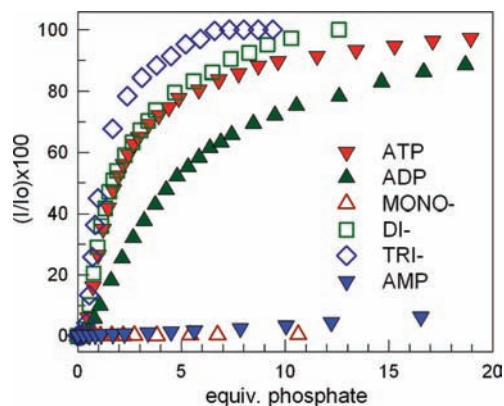


Figure 8. Spectrofluorimetric titration profiles obtained for different phosphates by monitoring the displacement of the indicator **6** from the receptor $[\text{Cu}_2^{\text{II}}(\mathbf{1})]^{4+}$. A 50:50 MeOH/H₂O solution (v/v) 2×10^{-5} M in $[\text{Cu}_2^{\text{II}}(\mathbf{1})]^{4+}$, 2×10^{-7} M in **6**, adjusted to pH 7 with HEPES buffer was titrated with a solution of the chosen phosphate. The emission intensity at 516 nm has been normalized with respect to the emission of the uncomplexed indicator.

polyphosphates, ADP and ATP. The results of pertinent titration experiments are illustrated in Figure 8. In particular, the following anions were considered: phosphate (MONO-), diphosphate (or pyrophosphate, DI-), triphosphate (TRI-), AMP, ADP, and ATP.

The titration profiles in Figure 8 show that phosphate affinity toward receptor $[\text{Cu}_2^{\text{II}}(\mathbf{1})]^{4+}$, expressed by the normalized fluorescent intensity of the displaced indicator (6-carboxyfluorescein), decreases along the series:



The same factors mentioned before ((i) nature of donor atoms and (ii) geometrical complementarity) should contribute to define the stability of the receptor-phosphate complex. However, in the present case contribution (i) should play a predominant role as both inorganic and nucleoside n -phosphates ($n = 2, 3$) offer two phosphonate oxygen atoms, which detain a definite negative charge. Then, triphosphates, due to their greater bite length, should encompass the intermetal distance better than diphosphates, which accounts for the higher affinity for the $[\text{Cu}_2^{\text{II}}(\mathbf{1})]^{4+}$ receptor. Moreover, within a given class of n -phosphates, nucleotides give less stable complex than inorganic phosphates, probably due to unfavorable steric effects exerted by the nucleoside appendage: thus, TRI- > ATP and DI- > ADP. Finally, the overall negative charge of the phosphate anion may play a further role, favoring the formation of the receptor-anion

complex: in particular, the negative charge is higher and the affinity for $[\text{Cu}_2^{\text{II}}(\mathbf{1})]^{4+}$ is larger (i) in inorganic phosphates with respect to nucleotides and (ii) in triphosphates with respect to diphosphates. The very poor ability to displace the fluorescent indicator does not allow a reliable comparison of orthophosphate and AMP. In any case, two oxygen atoms of the inorganic phosphate may have difficulty in encompassing the relative high $\text{Cu}^{\text{II}}-\text{Cu}^{\text{II}}$ distance, while AMP may bind a copper(II) center with an $-\text{NH}_2$ group of the adenine moiety (*vide supra*). Further studies are underway in our laboratory to better define the interactions between receptor $[\text{Cu}_2^{\text{II}}(\mathbf{1})]^{4+}$ and polyphosphates.

Summary and Conclusion

This work has demonstrated that the dimetallic cryptate $[\text{Cu}_2^{\text{II}}(\mathbf{1})]^{4+}$ exerts selective recognition of GMP with respect to other nucleoside monophosphates. Such a discriminating behavior has been tentatively ascribed to the capability of GMP to match, with its phosphonate and enolate oxygen atoms, the distance between the two Cu^{II} ions inside the cryptate. Recognition is effectively signaled through the displacement of the indicator 6-carboxyfluorescein, which releases its yellow fluorescent emission. A thorough analytical investigation evidenced the occurrence of several simultaneous equilibria involving 1:1 and 2:1 receptor/NMP and receptor/indicator complexes. Quite interestingly, in the experimental conditions chosen according to the employed sensing paradigm, the added analyte (NMP) displaces the indicator from the 2:1 receptor/indicator complex, while the 1:1 receptor/analyte inclusion complex forms. This highlights the significance of size and bond complementarity between receptor and analyte and encourages synthetic chemists to design of systems of enhanced recognition properties. Less attention has to be devoted to the choice of the indicator, whose interaction takes place out of the cavity and does not present pronounced elements of selectivity. Rigorously, such guidelines apply to cage-shaped receptors for anionic analytes.

Acknowledgment. The financial contributions from the Italian Ministry of University and Research (PRIN, FIRB) and from the University of Pavia (FAR) are gratefully acknowledged.

Supporting Information Available: Calculation details, spectrofluorimetric titration profiles for all nucleotides, EPR spectra, calculated ESI mass spectra, cyclic voltammetry profiles, and MM+ calculated structure of the receptor. This material is available free of charge via the Internet at <http://pubs.acs.org>.

JA9046262